Erschienen in: The Journal of Biological Chemistry ; 281 (2006), 29. - S. 20045-20054
https://dx.doi.org/10.1074/jbc.M603063200

THE JOURNAL OF BIOLOGICAL CHEMISTRY VOL. 281, NO. 29, pp. 20045–20054, July 21, 2006

The UBA Domains of NUB1L Are Required for Binding but Not for Accelerated Degradation of the Ubiquitin-like Modifier FAT10*

Received for publication, March 31, 2006, and in revised form, May 16, 2006 Published, JBC Papers in Press, May 17, 2006, DOI 10.1074/jbc.M603063200

Gunter Schmidtke, Birte Kalveram, Elvira Weber, Petra Bochtler[1], Sebastian Lukasiak, Mark Steffen Hipp[2], and Marcus Groettrup[3]

From the Division of Immunology, Department of Biology, University of Konstanz, Universitaetsstr. 10, D-78457 Konstanz, Germany

Proteins selected for degradation are labeled with multiple molecules of ubiquitin and are subsequently cleaved by the 26 S proteasome. A family of proteins containing at least one ubiquitin-associated (UBA) domain and one ubiquitin-like (UBL) domain have been shown to act as soluble ubiquitin receptors of the 26 S proteasome and introduce a new level of specificity into the degradation system. They bind ubiquitylated proteins via their UBA domains and the 26 S proteasome via their UBL domain and facilitate the contact between substrate and protease. NEDD8 ultimate buster-1 long (NUB1L) belongs to this class of proteins and contains one UBL and three UBA domains. We recently reported that NUB1L interacts with the ubiquitin-like modifier FAT10 and accelerates its degradation and that of its conjugates. Here we show that a deletion mutant of NUB1L lacking the UBL domain is still able to bind FAT10 but not the proteasome and no longer accelerates FAT10 degradation. A version of NUB1L lacking all three UBA domains, on the other hand, looses the ability to bind FAT10 but is still able to interact with the proteasome and accelerates the degradation of FAT10. The degradation of a FAT10 mutant containing only the C-terminal UBL domain is also still accelerated by NUB1L, even though the two proteins do not interact. In addition, we show that FAT10 and either one of its UBL domains alone can interact directly with the 26 S proteasome. We propose that NUB1L not only acts as a linker between the 26 S proteasome and ubiquitin-like proteins, but also as a facilitator of proteasomal degradation.

Ubiquitin, a small protein of 76 amino acids is one of the most conserved proteins known and has been found in all eukaryotic cells studied. It is essential for a variety of cellular processes, including degradation, cell-cycle regulation, DNA repair, stress response, embryogenesis, apoptosis, signal transduction, and transmembrane and vesicular transport (1–6). Throughout the past years, a family of proteins containing structural motives related to ubiquitin has been described that can be grouped into the ubiquitin-like modifiers and the ubiquitin-domain proteins (7). The ubiquitin-like modifiers have substantial sequence or structural homology to ubiquitin and form covalent conjugates with their target proteins. However, unlike ubiquitin, which can form large polymeric conjugates, usually only monomeric modifications are observed. As is the case for ubiquitin, a C-terminal diglycine motif is essential for conjugation of most modifiers to their target proteins (8). Prominent members of this group include SUMO-1, which serves several functions including nuclear transport and budding (9, 10), NEDD8, which regulates SCF ubiquitin-ligases via cullin modification (11), ISG15, which plays a role in innate immunity and in the response to α-interferon (12, 13), and FAT10, which is inducible with γ-interferon (IFN-γ[4] and tumor necrosis factor α (TNF-α) (14, 15), and has been shown to cause apoptosis upon ectopic expression (16).

The ubiquitin-like protein FAT10 consists of two UBL domains in a head to tail formation, which are about 29 and 36% identical to ubiquitin, respectively. Several key features of ubiquitin, like the lysine residues 48, 63, and 29, which are required for polyubiquitin chain formation, are conserved in both UBL domains (17). Its C terminus bears a free diglycine motif, which is necessary for the conjugation to so far unidentified target proteins (16). Like ubiquitin (18), FAT10 causes rapid degradation of long-lived proteins when fused to the N terminus (19). However, unlike ubiquitin, which is recycled from the degraded target proteins, FAT10 is digested along with its substrates. FAT10 thus has a relatively short half-life (20), which decreases dramatically by coexpression of a member of the group of ubiquitin-domain proteins named NEDD8 ultimate buster-1 long (NUB1L) (21, 22).

Several ubiquitin-domain proteins consist of an N-terminal UBL domain, which binds to the 19 S regulator of the 26 S proteasome (23) and one or more UBA domains that bind mono- or polyubiquitin (24, 25). Members of this group include Rad23, which is involved in nucleotide excision repair, and Dsk2, which plays a role in spindle pole duplication (26–28). It has been suggested that these ubiquitin-domain proteins serve as linkers of

* This work was supported by Deutsche Forschungsgemeinschaft Grants GR1517/2-1 and GR1517/3-1 and the Fritz Thyssen Foundation. The costs of publication of this article were defrayed in part by the payment of page charges. This article must therefore be hereby marked "*advertisement*" in accordance with 18 U.S.C. Section 1734 solely to indicate this fact.

[1] Present address: IZKF, Dept. of Internal Medicine I, University of Ulm, D-89081 Ulm, Germany.

[2] Present address: Dept. of Biological Sciences, Stanford University, Stanford, CA 94305.

[3] To whom correspondence should be addressed. Tel.: 49-7531-88-2130; Fax: 49-7531-88-3102; E-mail: marcus.groettrup@uni-konstanz.de.

[4] The abbreviations used are: IFN, interferon; GST, glutathione *S*-transferase; HA, hemagglutinin; NEDD, neural precursor cell-expressed developmentally down-regulated; NUB1, NEDD8 ultimate buster-1; UBA domain, ubiquitin-associated domain; TNF, tumor necrosis factor; GFP, green fluorescent protein; UBL domain, ubiquitin-like domain; DHFR, dihydrofolate reductase.

ubiquitylated proteins and the 26 S proteasome (29), but the role of these proteins in degradation is still controversial. Some artificial reporter substrates accumulate in rad23-deleted and dsk2-deleted cells, as do high molecular weight ubiquitin conjugates (30–34), but even in rad23/rpn10 doubly deleted cells, the bulk turnover of short-lived proteins is not affected (35). Overexpression of either hPlic or Rad23 leads to inhibition of substrate turnover by the 26 S proteasome (36, 37), and an excess of Rad23 inhibits the *in vitro* degradation of Ub_5DHFR by the 26 S proteasome (38). A recent study suggested that UBL-UBA proteins, acting as multiubiquitin chain-binding proteins, define a new layer of substrate specificity, where different multiubiquitin chain-binding proteins are involved in the degradation of different proteins (39). The UBA domains are usually essential for this function. Rad23 lacking its UBA domains cannot inhibit degradation *in vitro* anymore (38), nor can it bind polyubiquitin. The UBL domains, on the other hand, are required for binding to the 26 S proteasome (23). For example, only Rad23 with both UBA and UBL domains can rescue degradation by either Rad23- or Rpn10-depleted proteasomes *in vitro* (39).

In this study we investigated the impact of the UBL and UBA domains of NUB1L on the binding and degradation of FAT10 as well as the role of the two UBL domains of FAT10. We were able to show that all three UBA domains of NUB1L are required for FAT10 binding, whereas the NUB1L UBL domain mediates interaction with the 26 S proteasome. Surprisingly, a NUB1L mutant lacking the UBA domains was still able to accelerate the degradation of FAT10, even though the two proteins no longer interacted. This apparent contradiction could be reconciled by the finding that FAT10 and NUB1L as well as both UBL domains of FAT10 separately interacted with the 26 S proteasome. Taken together, we found no correlation between the binding of target proteins to NUB1L and the ability of NUB1L to accelerate their degradation, suggesting that NUB1L, by binding to the proteasome via its UBL domain, functions as a facilitator of proteasomal degradation of FAT10 without the necessity to serve as a linker.

EXPERIMENTAL PROCEDURES

Antibodies—The anti-HA monoclonal antibody clone HA7 (Sigma) was used for immunoprecipitation in Figs. 2–7 and for the Western blot in Fig. 8*A*. The anti-His_6 monoclonal antibody clone BMG His-1 (Roche Diagnostics) was used for immunoprecipitation shown in Figs. 2, *B* and *D*, and 4*D*. A mixture of monoclonal anti-green fluorescent protein (GFP) clones 7.1 and 13.1 (Roche Diagnostics) was used for the immunoprecipitation in Fig. 6*A* and for the Western blot in Fig. 8*B*. An anti-HA monoclonal antibody clone HA7 antibody peroxidase conjugate (Sigma) was used for the Western blot shown in Fig. 8*C*, and a polyclonal rabbit anti-GFP antibody (Sigma) for the Western blot in Fig. 8*D*. The Western blots presented in Fig. 8, *E* and *F*, were performed with a rabbit polyclonal anti-Rpt6 (S8) from Biomol (Exeter, UK). The immunoprecipitation of the proteasome was performed with 5 μl of ascitis fluid of the anti-HN3 antibody MCP444 (40). The mouse monoclonal anti-iota antibody 27K was kindly provided by Dr. Klaus Scherrer (Paris). Anti-FAT10 antibody has been described (19), anti-NUB1 antibody was a gift from Dr. Michael E. Cheetmham (London). The anti-glyceraldehyde-3-phosphate dehydrogenase antibody was purchased from Ambion, Inc. (Austin, TX). All antibodies were coupled to EZview Red Protein A or G Affinity Gel (Sigma) for immunoprecipitation. All horseradish peroxidase-conjugated secondary antibodies were purchased from DAKO (Glostrup, Denmark).

Tissue Culture—HEK293T and HeLa cells were kept in Iscove's modified Dulbecco's medium. Induction of FAT10 and NUB1L was performed by overnight incubation with IFN-γ (Endogen, Rockford, IL) at a final concentration of 200 units/ml and TNF-α (Endogen) at 400 units/ml.

Quantitative Reverse Transcriptase-PCR—The RNA was isolated with a kit from Machery Nagel (Düren, Germany) and the cDNA was generated with a kit from Promega according to the instructions of the manufacturer. We used the following primers and conditions: for FAT10 forward primer, ttgttcttgtggagtcaggtg; reverse primer, agtaagttgccctttctgatgc, with cycling parameters at 95 °C for 10 min, 95 °C for 15 s, 60 °C for 5 s, 72 °C for 9 s, 40 times; for NUB1L forward primer: aaagggatgggctactccac, reverse primer, cgtctgttgaggcactagagg with cycling parameters at 95 °C for 10 min, 95 °C for 15 s, 60 °C for 5 s, 72 °C for 13 s, 40 times; for glyceraldehyde-3-phosphate dehydrogenase forward primer: gaaggtgaaggtcggagtc, reverse primer, gaagatggtgatgggatttc, with cycling parameters at 95 °C for 10 min, 95 °C for 15 s, 60 °C for 5 s, 72 °C for 11 s, 40 times.

Generation of cDNA Constructs—The generation of HA-NUB1L (Figs. 1–6) and His_6-FAT10 (Fig. 2) both in pcDNA3.1, HA-FAT10 in pBI, HA-FAT10 in pBI + GFP, HA-NUB1L in pBI + GFP, HA-FAT10 + HA-NUB1L in pBI, FAT10-GFP, SUMO-1-GFP, and GST-FAT10 have been described (20). The glutathione *S*-transferase (GST)-expressing vector pGEX-4T-3 and the GFP-expressing vector pN1EGFP are commercially available from Amersham Biosciences and Clontech. Generation of expression constructs for NUB1LΔUBA1, NUB1LΔUBA2, NUB1LΔUBA3, NUB1LΔUBA1/2, NUB1LΔUBA1/3, NUB1LΔUBA2/3, NUB1LΔUBA1–3, NUB1LΔUBL, and NUB1 was performed by PCR. A list of the primers used will be available on request. First we made the deletion mutant NUB1LΔUBA1–3. The parts of the DNA from the 5′-end of the full-length cDNA to the 5′-end of UBA1, and from the 3′-end of UBA3 to the 3′-end of the wild-type cDNA were amplified separately by PCR. A short overlap of the primers flanking the region to be deleted allowed for assembly of these two fragments that were completed by amplification using the 5′ and 3′ primers of the full-length cDNA. The short overlap of the two primers contained three unique restriction sites, which were introduced by conservative mutations. The UBA domain or domains of the other mutants were amplified by PCR and introduced into NUB1LΔUBA1–3 via the unique restriction sites. NUB1LΔUBL was generated the same way as NUB1LΔUBA1–3, but different primers were used. FAT10-N-GFP and FAT10-C-GFP were generated by PCR amplification of the N-terminal (FAT-N-GFP) or C-terminal (FAT10-C-GFP) UBL domain of FAT10 and replacing FAT10 in a FAT10-GFP expressing vector by restriction digestion. The two domains were cloned into pcDNA3.1 as well. All sequences were verified by sequencing.

Immunoprecipitation—Co-immunoprecipitation of NUB1L mutants and His_6-FAT10, and NUB1L and FAT10 mutants was

performed as previously described (20). For the immunoprecipitation of the 26 S proteasome, one well of a 6-well plate of transfected cells was used per immunoprecipitation. Cells were lysed in 25 mM Tris, pH 7.8, 2 mM $MgCl_2$, 20% glycerol, 1 mM dithiothreitol, and 2 mM ATP by sonification. After centrifugation for 15 min at 20,000 × *g*, the supernatant was supplemented with bovine serum albumin to a final concentration of 1 mg/ml, 15 mM creatine phosphate, and 15 units/ml creatine kinase. After preincubation of the lysates for 1 h with Sepharose CL-4B (Amersham Biosciences), the supernatant was immunoprecipitated for 4 h with 5 μl of MCP444 ascitis fluid. After washing three times with lysis buffer, the matrix was washed once with 25 mM Tris, pH 7.8, 2 mM $MgCl_2$, 20% glycerol, 1 mM dithiothreitol, 2 mM ATP, 150 mM KCl, and 0.05% Triton X-100. Bound proteins were eluted by boiling in SDS sample buffer and analyzed by Western blotting.

Pulse-Chase Experiments—Tissue culture and transfection of HEK293T cells, metabolic labeling, and pulse-chase analysis were performed as described (20).

GST Pulldown Assays—Glutathione-Sepharose 4B (Amersham Biosciences) and recombinant GST or GST-FAT10 (purified as previously described (20)) were incubated overnight at 4 °C with 20 μg of 26 S proteasome in the presence or absence of recombinant His_6-NUB1L (purified as previously described (20)). The incubation buffer contained 20% glycerol, 2 mM ATP, 1 mM dithiothreitol, and 100 μM *N*-acetyl-Leu-Leu-nor leucinal (Roche Diagnostics). The matrix was washed four times with incubation buffer and analyzed by Western analysis for the 20 S subunit iota. All other GST pulldown assays and coupled *in vitro* transcription/translation reactions were performed as described (20).

Purification of 26 S Proteasomes—Purification of 26 S proteasomes was performed as detailed elsewhere (41).

Analysis of Intracellular Protein Degradation and Proteasome Activity—The experiments were performed exactly as previously described (42).

RESULTS

All Three UBA Domains of NUB1L Are Required for the Interaction with FAT10, but the UBL Domain Is Dispensable—We recently showed that NUB1L interacts with FAT10 and accelerates its degradation and that of FAT10-conjugated proteins (19, 20). To elucidate the role of the different UBL and UBA domains, we created several deletion mutants of NUB1L. It should be pointed out that NUB1 is a natural splicing variant of NUB1L, which has a deletion of 14 amino acids, encompassing the C-terminal third of a UBA domain (UBA2 in Fig. 1) (43). This flexibility in the structure should allow us to remove all three UBA domains together (NUB1LΔUBA1–3), or two of them (NUB1LΔUBA2/3, NUB1LΔUBA1/3, and NUB1LΔUBA2/3) or only one of them (NUB1LΔUBA3, NUB1LΔUBA2, and NUB1LΔUBA1) without compromising the folding. We also deleted the ubiquitin-like domain (NUB1LΔUBL) as indicated in Fig. 1. First we analyzed the interaction of FAT10 and NUB1L mutants *in vitro*. After *in vitro* transcription and translation 10% of the reactions were analyzed by SDS-PAGE and autoradiography. All analyzed mutants appeared as a single band and were expressed as soluble proteins in amounts comparable with wild-type NUB1L (Fig. 1*B*). Half of the

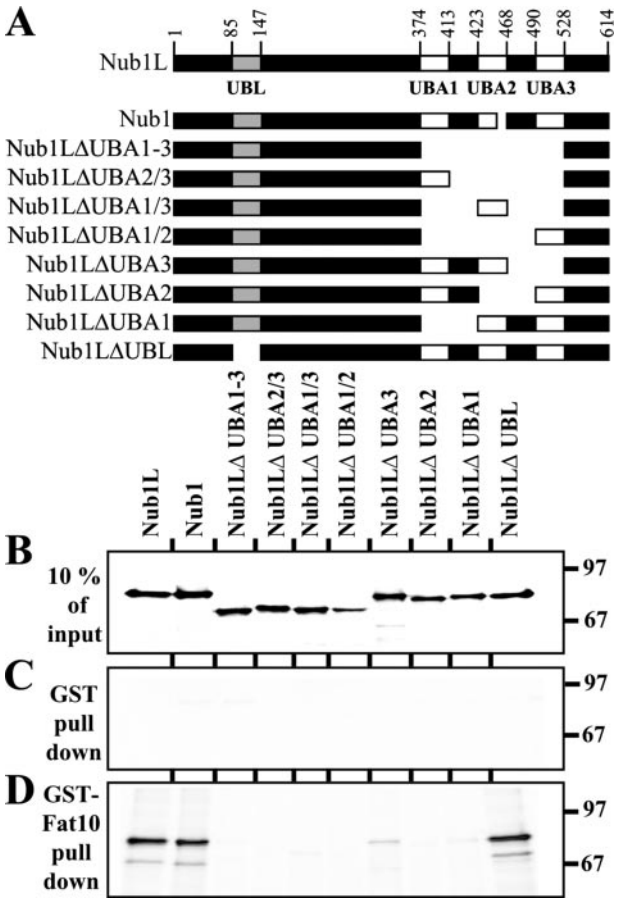

FIGURE 1. **Domain structure of NUB1 and NUB1L, some deletion mutants, and their interaction with GST and GST-FAT10.** *A*, the positions of the domains of NUB1L are indicated by the number of the amino acids. The UBL domains are shown in *gray*, the UBA domains are shown in *white*. *B*, autoradiography of *in vitro* transcribed and translated NUB1L mutants after separation by SDS-PAGE. A 10% aliquot of each reaction was loaded to demonstrate the amount available for the GST pulldown. The positions of molecular mass markers (in kDa) are indicated on the *right*. *C*, autoradiography of the NUB1L mutants shown in *A* after incubation with GST-coupled GSH-Sepharose, washing, and separation by SDS-PAGE. The lane occupation is the same as in *B*. *D*, autoradiography of the NUB1L mutants shown in *A* after incubation with GST-FAT10-coupled GSH-Sepharose, washing, and separation by SDS-PAGE. Lane occupation is the same as in *B*. Only wild-type NUB1L, NUB1, and NUB1LΔUBL interact strongly, NUB1LΔUBA3 interacts weakly with GST-FAT10. The experiments were repeated three times with similar outcomes.

remainder of the reaction was incubated with GST coupled to glutathione (GSH)-Sepharose, the other half was incubated with GST-FAT10 coupled to GSH-Sepharose. After washing, the bound proteins were analyzed by SDS-PAGE and autoradiography. None of the analyzed proteins could be detected after pulldown with GST alone (Fig. 1*C*). Only wild-type NUB1L, NUB1, and NUB1LΔUBL were pulled down in significant amounts by GST-FAT10. NUB1LΔUBA3 was also bound, but to a much lesser extent, whereas none of the other mutants interacted with GST-FAT10 in this assay (Fig. 1*D*).

To study the interaction of FAT10 and NUB1L *in vivo*, we transfected wild-type and mutant HA-NUB1L either alone or together with His_6-tagged FAT10 into HEK293T cells. After metabolic labeling with [^{35}S]methionine, the cells were lysed and subjected to immunoprecipitation with anti-HA antibodies. The recovered proteins were separated by SDS-PAGE and analyzed by autoradiography. As can be seen in Figs. 2, *A* and *C*,

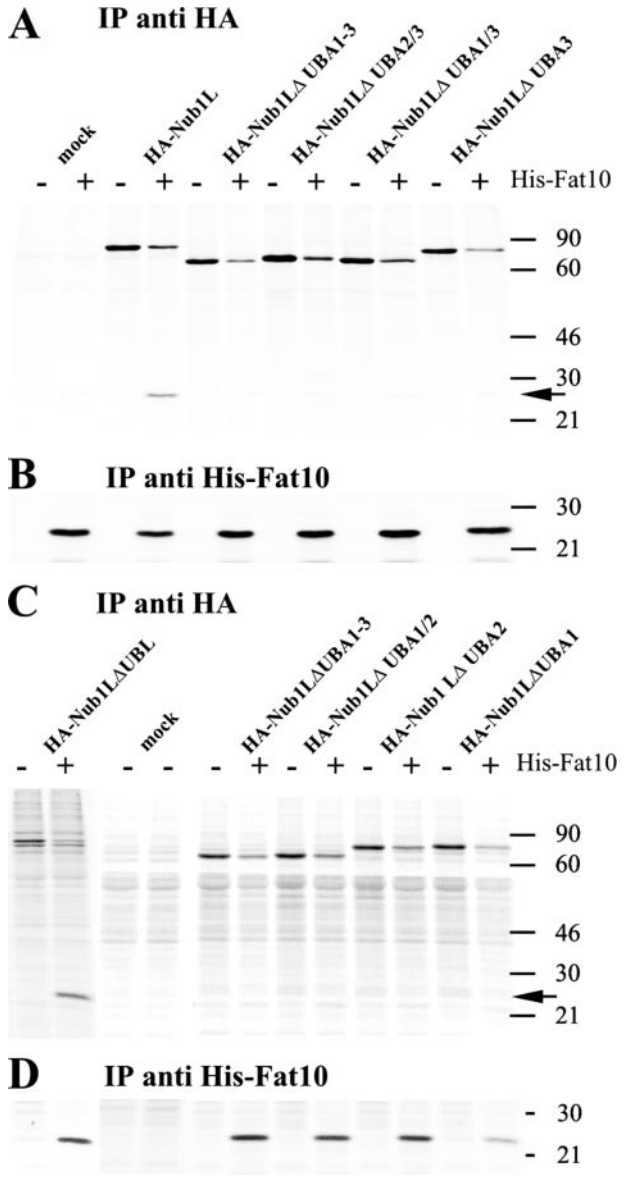

FIGURE 2. **Co-immunoprecipitation of NUB1L mutants and FAT10.** *A* and *C*, empty vector (mock) or HA-tagged NUB1L mutants lacking one or more domains were transfected either alone (− *His-FAT10*) or together with His_6-tagged FAT10 (+ *His-FAT10*) into HEK293T cells. The cells were lysed and an anti-HA immunoprecipitation (*IP*) was performed. The proteins bound by the antibody were separated by SDS-PAGE and analyzed by autoradiography. The NUB1L mutants appear between the 60- and 90-kDa molecular mass markers indicated at the *right*. An *arrow* on the *right* of the gel denotes the position of co-immunoprecipitated (*IP*) FAT10. Only wild-type HA-NUB1L and HA-NUB1LΔUBL coprecipitated significant amounts of His_6-FAT10. *B* and *D*, to analyze the amount of FAT10 available, the supernatants after the immunoprecipitations shown in *A* and *C* were precipitated with anti-His_6 antibodies, and the bound proteins were separated by SDS-PAGE. Lane occupation is the same as in *A* and *C*, respectively. His_6-FAT10 was present in all FAT10-transfected cells. The experiments were repeated three times yielding similar results.

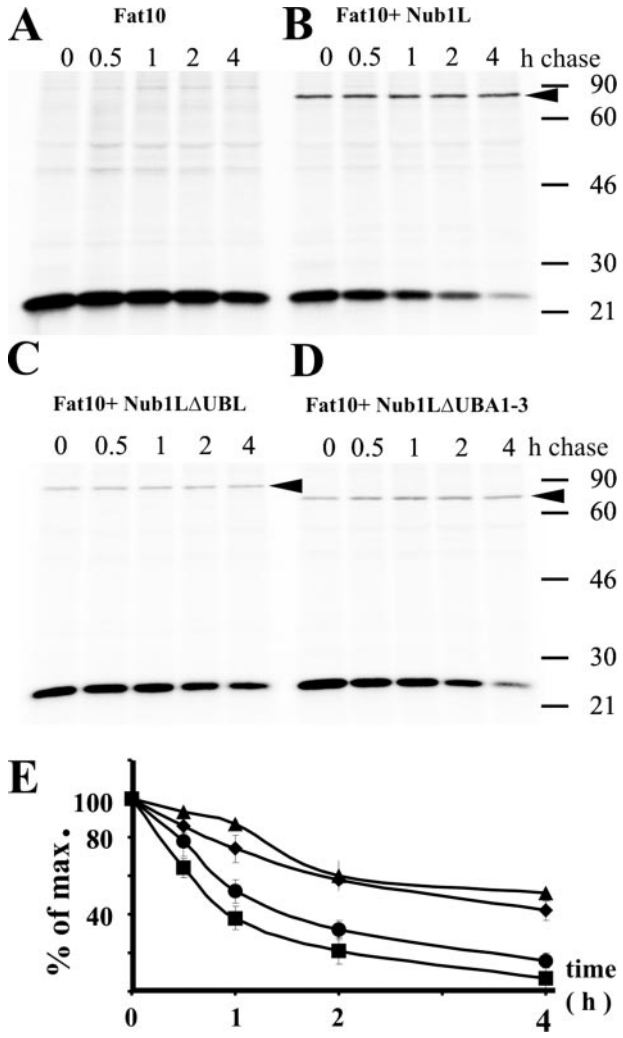

FIGURE 3. **Accelerated degradation of FAT10 by NUB1L and NUB1LΔUBA1–3, but not by NUB1LΔUBL.** *A*, pulse-chase analysis of FAT10 degradation. HEK293T cells were transfected with HA-FAT10 and labeled with [^{35}S]methionine. At the indicated time points of chase, aliquots of the cells were lysed and anti-HA immunoprecipitations were performed. Bound proteins were analyzed by SDS-PAGE and autoradiography. *B*, same as in *A*, but HA-NUB1L was cotransfected. A *closed arrow* at the *right* of the gel denotes the position of NUB1L. Positions of molecular weight markers from 21 to 90 kDa are at the *right* of the gel. *C*, same as in *A*, but HA-NUB1LΔUBL was cotransfected. *D*, same as in *A*, but HA-NUB1LΔUBA1–3 was cotransfected. *E*, graphic representation of degradation rates as determined for FAT10 alone in *A* (*diamonds*), with NUB1L in *B* (*squares*), with NUB1LΔUBL in *C* (*triangles*), and with NUB1LΔUBA1–3 in *D* (*filled circles*). The amount of radioactivity recovered at 0 h was set to 100%. The activity immunoprecipitated at 0.5, 1, 2, and 4 h was calculated relative to the 0 h value. Values represent the mean of five independent experiments ± S.E.

and 4*C*, only wild-type NUB1L, NUB1, and NUB1LΔUBL were able to pull down His_6-FAT10 from the lysates. A subsequent immunoprecipitation of the supernatants with anti-His_6 antibody demonstrated that sufficient His_6-FAT10 was available in all reactions, so lack of expression can be excluded as a reason for the negative results. From the experiments presented in Figs. 1, 2, and 4, *C* and *D*, we conclude that the interaction of FAT10 and NUB1L depends on the presence of all three UBA domains, but is independent of the UBL domain of NUB1L. The deletion of only 14 amino acids in NUB1, which is about one-third of the UBA2 domain is not sufficient to abrogate the interaction of NUB1 and FAT10.

Only the UBL Domain of NUB1L Is Essential for the Accelerated Degradation of FAT10—To analyze the impact of the UBA and UBL domains of NUB1L on the accelerated degradation of FAT10, we cotransfected NUB1LΔUBA1–3 and NUB1LΔUBL together with FAT10 in HEK293T cells and determined the half-life of FAT10 by pulse-chase analysis. For comparison, we also transfected FAT10 alone and in combination with wild-

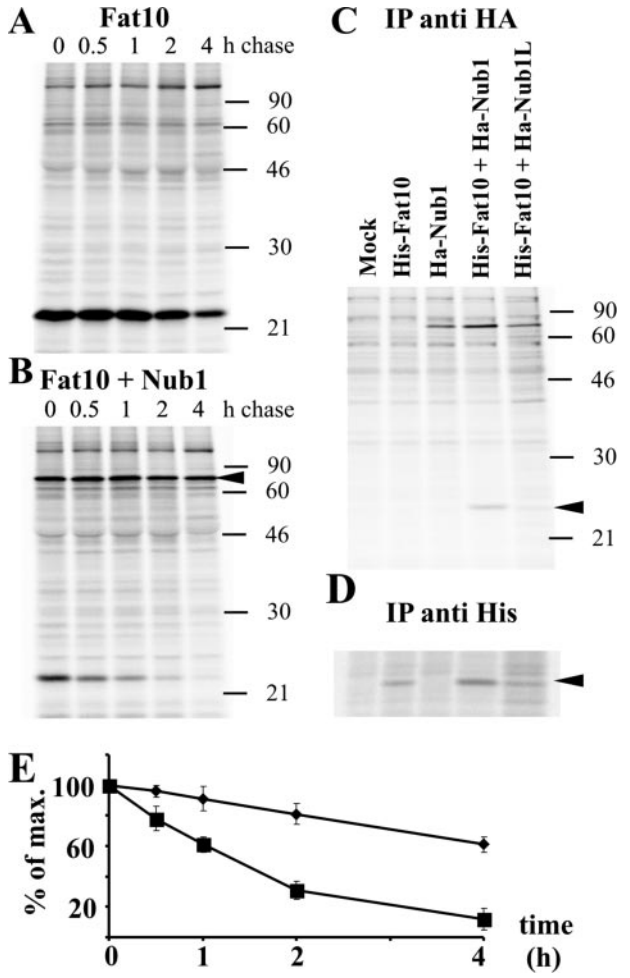

FIGURE 4. **NUB1 interacts with FAT10 and accelerates its degradation.** *A*, HEK293 T cells were transiently transfected with HA-FAT10. After pulse labeling with [^{35}S]methionine, aliquots of the cells were harvested at the indicated time points of chase, lysed, and anti-HA immunoprecipitations (*IP*) were performed. Bound proteins were analyzed by SDS-PAGE and autoradiography. *B*, same as in *A*, but NUB1 was coexpressed. The position of NUB1 is indicated by an *arrowhead*. Molecular mass markers (in kDa) are shown at the *right*. *C*, co-immunoprecipitation of HA-NUB1 and His-FAT10. Empty vector (mock), or His-FAT10 or HA-tagged NUB1 were transfected either alone or together (*His-FAT10 + HA-NUB1*) into HEK293T cells. As a positive control we used His-FAT10 and HA-NUB1L. The cells were lysed and an anti-HA immunoprecipitation was performed. The proteins bound by the antibody were separated by SDS-PAGE and analyzed by autoradiography. An *arrowhead* on the *right* of the gel denotes the position of co-immunoprecipitated FAT10. *D*, the supernatants of *C* were immunoprecipitated with anti-His$_6$ antibodies to show the amount of FAT10 available, the position of which is indicated by an *arrowhead*. *E*, graphic evaluation of the different degradation rates of FAT10 as determined in *A* (*diamonds*) and *B* (*squares*).

type NUB1L (Fig. 3). As seen in Fig. 3, *A* and *B*, wild-type NUB1L accelerates the degradation of FAT10 by a factor of about 4, which is consistent with our results previously obtained in HeLa cells (20). In contrast, the cotransfection of NUB1LΔUBL did not have an effect on the half-life of FAT10 (compare Fig. 3, *A* and *C*). Unexpectedly, the cotransfection of NUB1LΔUBA1–3, which does not interact with FAT10, accelerated the degradation of FAT10 almost as potently as wild-type NUB1L (compare Fig. 3, *B* and *D*, for quantifications on a radioimager see Fig. 3*E*). We also analyzed the impact of the small splicing variant NUB1 on FAT10 degradation. We found that NUB1 is able to accelerate the degradation of FAT10 as potently as NUB1L (Fig. 4).

NUB1L Does Not Influence Protein Degradation in General—We already published that expression of NUB1L does not have any effect on the degradation of the model substrates ubiquitin-GFP and ubiquitin-DHFR (19). To extend this study and investigate the role of NUB1L in proteasome-dependent protein degradation we analyzed the degradation of short lived proteins in mock transfected cells and NUB1L-transfected cells. Western blot analysis of lysates from these cells showed a clear overexpression of NUB1L in the NUB1L transfectant (Fig. 5*A*). Aliquots of these cells were labeled with [^{35}S]methionine, washed, and chased for 1 h. After this incubation cells were treated with trichloroacetic acid, and the acid-soluble radioactivity, representing the amount of degraded protein, was counted. Mock transfected cells converted 31% (±5%) and NUB1L transfected cells 27% (±4%) of the activity into acid soluble counts. The ubiquitin-proteasome system is responsible for degradation of about 75% of bulk cellular proteins occurring within 1 h after synthesis. Hence, a major effect of NUB1L overexpression on degradation by the ubiquitin-proteasome system should have been detectable in this assay. Because this was not the case, NUB1L is unlikely to generally affect ubiquitin-mediated degradation. Moreover, the intracellular proteasome activity as measured by degradation of the cell-permeable fluorogenic proteasome substrate MeO-Suc-GLF-AMC was not affected by NUB1L overexpression.

Treatment with IFN-γ and TNF-α Enhances the Expression of NUB1L and Degradation of Endogenous FAT10—Next we investigated whether the endogenous up-regulation of NUB1L expression by TNF-α and IFN-γ suffices to accelerate the degradation of endogenous FAT10. The combined treatment of HeLa cells with IFN-γ and TNF-α for 1 day resulted in an over 9-fold increase in FAT10 mRNA expression and over 5-fold increase in NUB1L mRNA expression as determined by quantitative reverse transcriptase PCR (Fig. 5*C*). Also on the protein level we detected an up-regulation of NUB1L by Western analysis (Fig. 5*B*). The degradation rate of endogenous FAT10 was then analyzed by pulse-chase analysis using an anti-FAT10 antibody. As shown in Fig. 5, *E* and *F*, FAT10 degradation was accelerated 3-fold as compared with FAT10-transfected HeLa cells without cytokine-mediated NUB1L induction (Fig. 5*D*). Transient FAT10 transfection of unstimulated HeLa cells was necessary because in the absence of cytokine stimulation no FAT10 protein was detectable. Taken together, we find a 3-fold acceleration of FAT10 degradation in cytokine-treated cells that correlates with an up-regulation of NUB1L.

The N-terminal UBL Domain of FAT10 Is Sufficient for Interaction with NUB1L—We previously reported that the interaction of NUB1L with FAT10 is specific for this protein, because binding of NUB1L to NEDD8, SUMO-1, and ubiquitin was not detected by co-immunoprecipitation (20). FAT10 consists of two ubiquitin-like domains in tandem array (44). To determine whether the N- and C-terminal domains can interact with NUB1L independently, we performed co-immunoprecipitation experiments. However, the persistence of these single UBL proteins was so short that we could only detect them in the presence of proteasome inhibitors (data not shown). To overcome this obstacle, we fused each of them to the N terminus of GFP, as we did for FAT10 as positive and SUMO-1 as negative con-

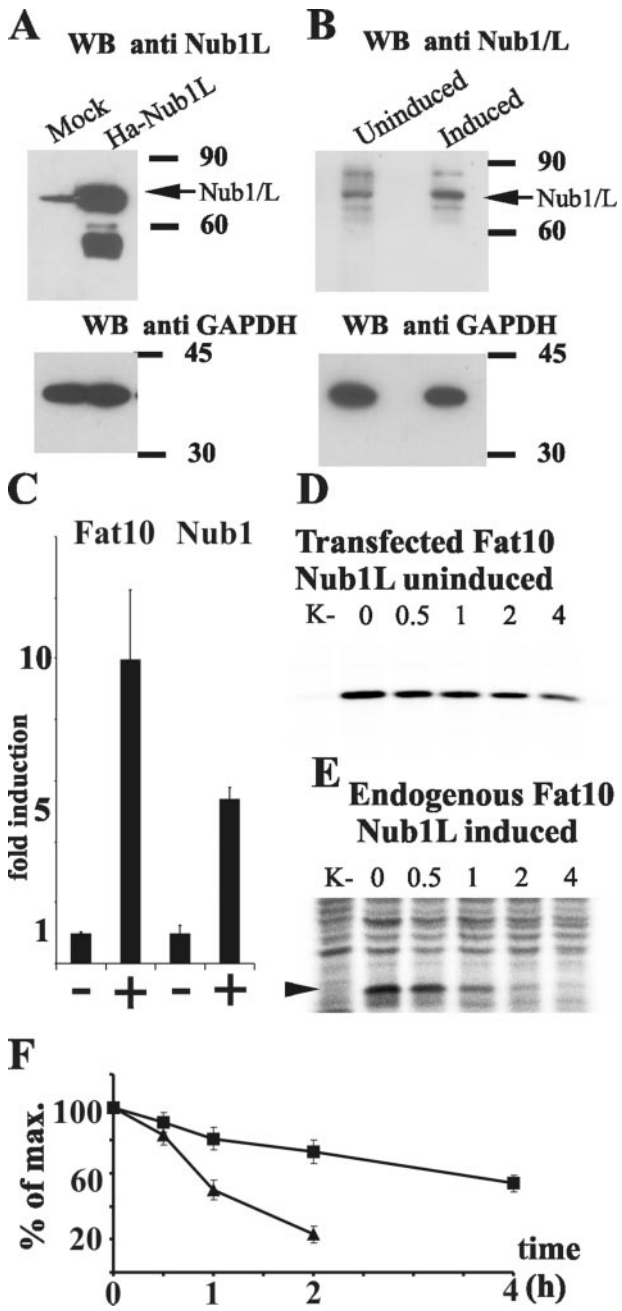

FIGURE 5. **Treatment with IFN-γ and TNF-α up-regulates NUB1L expression and accelerates the degradation of FAT10.** *A*, anti-NUB1L Western blot (*WB*) of lysates from mock transfected and HA-NUB1-transfected HEK293T cells (*top panel*), Western analysis of glyceraldehyde-3-phosphate dehydrogenase (*GAPDH*) protein is used as loading control (*bottom panel*). *B*, anti-NUB1L Western blot of lysates from untreated HeLa cells and HeLa cells induced with IFN-γ and TNF-α for 1 day. An *arrow* at the *right* indicates the position of NUB1L (*top panel*); the same lysates probed with anti-glyceraldehyde-3-phosphate dehydrogenase antibodies serves as loading control (*bottom panel*). *C*, real time RT-PCR analysis of FAT10 and NUB1L mRNA expression in HeLa cells before (−) and after (+) treatment with TNF-α and IFN-γ for 1 day. *D*, HeLa cells were transfected with an HA-FAT10 expression construct and the degradation rate of FAT10 was determined in a pulse-chase experiment. *K*− denotes an immunoprecipitation with irrelevant antibody. *E*, analysis of the degradation rate of endogenous FAT10 after induction of FAT10 and NUB1L by IFN-γ and TNF-α. The pulse-chase experiment was performed as in *E* using an anti-FAT10 antibody. *K*− is an immunoprecipitation with preimmune serum. The position of FAT10 is indicated by an *arrowhead*. *F*, graphic evaluation of the different degradation profiles of FAT10 as determined in *D* (*squares*) and *E* (*triangles*).

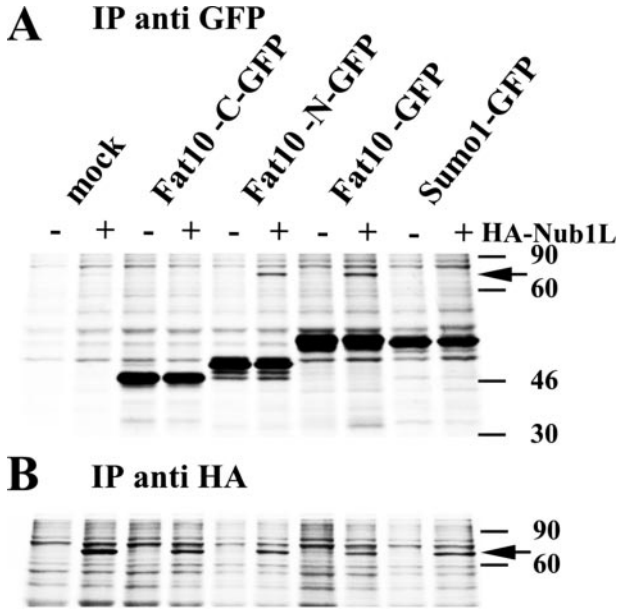

FIGURE 6. **The N-terminal, but not the C-terminal UBL domain of FAT10 interacts with NUB1L.** *A*, empty vector (*mock*), the C-terminal UBL domain of FAT10 (*FAT10-C*), the N-terminal UBL domain of FAT10 (*FAT10-N*), wild-type FAT10 as positive- and SUMO-1 as negative control, all as GFP fusions, were transfected either alone (−*HA-NUB1L*) or together with HA-tagged NUB1L (+*HA-NUB1L*) into HEK293T cells. The cells were lysed and an anti-GFP immunoprecipitation (*IP*) was performed. The proteins bound by the antibody were separated by SDS-PAGE and analyzed by autoradiography. An *arrow* denotes the position of NUB1L. Molecular weight markers are shown at the *right*. *B*, to analyze the amount of NUB1L available, the supernatants after the immunoprecipitation shown in *A* were precipitated with anti-HA antibodies, and the bound proteins were separated by SDS-PAGE. Lane occupation is the same as in *A*. An *arrow* denotes the position of NUB1L. HA-NUB1L was present in all HA-NUB1L-transfected cells. The experiments were repeated two times with similar outcomes.

trol (Fig. 6). Mock transfected cells, or cells transfected with the constructs mentioned above either alone or together with HA-NUB1L were metabolically labeled, lysed, and subjected to anti-GFP immunoprecipitation. After washing, the bound proteins were analyzed by SDS-PAGE and autoradiography. The supernatants of this first precipitation were then subjected to immunoprecipitation with anti-HA antibodies to determine the level of NUB1L expression. As shown in Fig. 6*A*, only the N-terminal UBL domain of FAT10 (FAT10-N-GFP) and FAT10-GFP coprecipitated NUB1L. There was no NUB1L signal in mock transfected cells and cells expressing SUMO-1-GFP or the C-terminal UBL domain of FAT10 (FAT10-C-GFP). Fig. 6*B* demonstrates that the amounts of NUB1L available were sufficient in all co-expression reactions to allow detection if bound to the respective GFP fusion protein.

NUB1L Accelerates Both FAT10-N-GFP and FAT10-C-GFP Degradation—To analyze the impact of NUB1L expression on the half-lives of the two isolated UBL domains of FAT10, we first determined the rate of degradation of FAT10-N-GFP and FAT10-C-GFP alone. As can be seen in Fig. 7, *A* and *B*, the degradation rates of the two UBL domain-GFP fusion proteins in HEK293T cells were significantly different from each other. FAT10-C-GFP was degraded with a rate comparable with that of wild-type FAT10-GFP (19) but slower than FAT10 itself (compare Figs. 3*E* and 7*I*). FAT10-N-GFP, in comparison, is a stable protein showing only minimal degradation within 5 h.

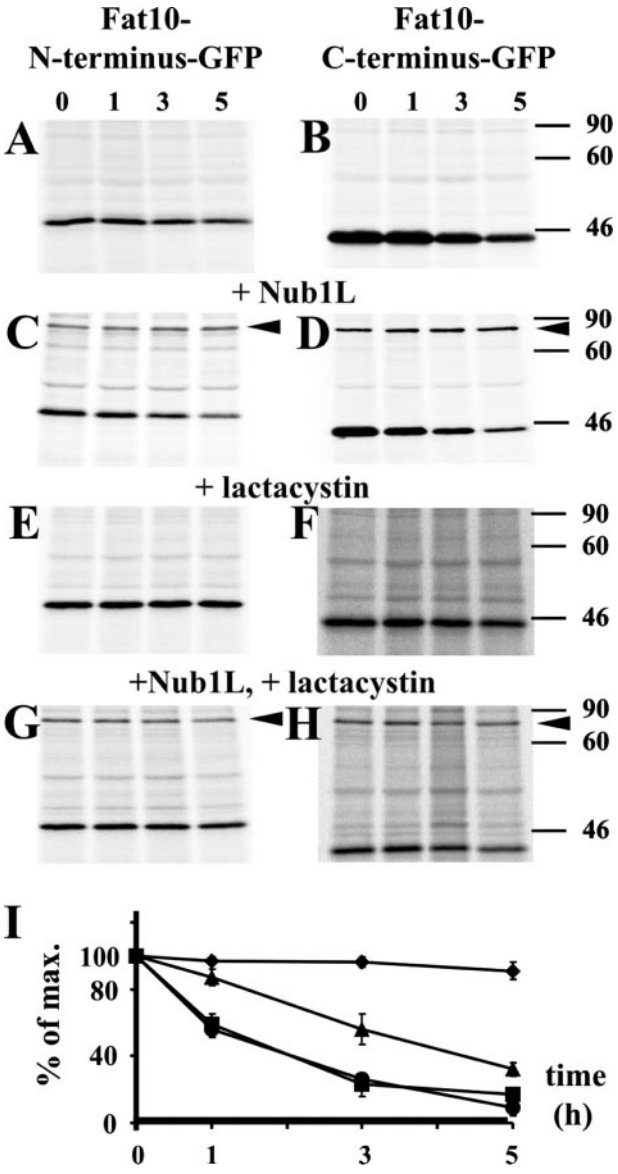

FIGURE 7. **Accelerated degradation of the FAT10 UBL domain-GFP fusion proteins by NUB1L.** *A*, pulse-chase analysis of the FAT10-N-terminal UBL domain fused to GFP. HEK293T cells were transfected with HA-FAT10-N terminus-GFP and labeled with [^{35}S]methionine. After the indicated time periods of chase, aliquots of the cells were lysed and anti-HA immunoprecipitations were performed. Bound proteins were analyzed by autoradiography after SDS-PAGE. An *arrowhead* at the *right* denotes the position of the GFP fusion proteins. *B*, same experimental setup as in *A*, but HA-FAT10-C terminus-GFP was transfected. The positions of the molecular weight markers are shown on the *right*. *C*, same as in *A*, but HA-NUB1L was cotransfected. *D*, same as in *B*, but HA-NUB1L was cotransfected. An *open arrow* at the *right* indicates the position of NUB1L. *E* and *F*, experiments were performed as in *A* and *B*, but in the presence of 50 μM lactacystin. *G* and *H*, experiments were performed as in *C* and *D*, but in the presence of 50 μM lactacystin. *I*, graphic representation of degradation rates as determined for FAT10-N terminus-GFP alone in *A* (*diamonds*), for FAT10-C terminus-GFP in *B* (*triangles*), for FAT10-N terminus-GFP with NUB1L in *C* (*squares*), and for FAT10-C terminus-GFP with NUB1L in *D* (*closed circles*). The amount of radioactivity recovered at 0 h was set to 100%. The activity immunoprecipitated at 1, 3, and 5 h was calculated relative to the 0 h value. Values represent the mean of three experiments ± S.E.

Co-expression of NUB1L lead to degradation of both UBL domain-GFP fusion proteins at almost the same rate (Fig. 7, *C*, *D*, and *I*). In the presence of NUB1L, FAT10-C-GFP degradation was accelerated by a factor of two to three. The enhancement in FAT10-N-GFP degradation caused by NUB1L was much higher, as it was degraded very slowly alone. To determine whether the degradation of FAT10-N-GFP and FAT10-C-GFP is mediated by the proteasome and not by another protease, we repeated the experiments in the presence of the proteasome inhibitor lactacystin. As shown in Fig. 7, *E* and *F*, both UBL domain-GFP fusion proteins were not degraded at all. Even co-expression of NUB1L did not lead to detectable degradation of either protein in the presence of lactacystin.

FAT10 and NUB1L Interact with the 26 S Proteasome—To investigate why NUB1LΔUBA1–3, but not NUB1LΔUBL, is able to accelerate the degradation of FAT10, we tested the working hypothesis that FAT10 may interact directly with the proteasome and that NUB1L with its UBL domain serves as a facilitator of degradation of FAT10 by the 26 S proteasome. Binding of NUB1 to the S5a (Rpn10) subunit of the 26 S proteasome has been shown *in vitro* before, as well as detection of NUB1 in preparations of purified 26 S proteasome (21). We decided to use co-immunoprecipitation from transfected HEK293T cells to determine whether FAT10, NUB1L, and their mutants are able to interact with the 26 S proteasome. We used a bi-directional vector expressing GFP from one side, and FAT10 or NUB1L from the other site of the promoter. Aliquots of lysates from transfected cells were analyzed for expression of the respective proteins (Fig. 8*A*, *lanes 2* and *3* for NUB1L and FAT10, and Fig. 6*B*, *lanes 5* and *6* for GFP). After immunoprecipitation with the monoclonal antibody MCP444 specific for the β-type proteasome core subunit HN3 (β7), we looked for coprecipitation of the expressed proteins with the proteasome. FAT10 and NUB1L, but not GFP, were co-immunoprecipitated by MCP444, indicating the specificity of the interaction (Fig. 8*C*, *lanes 2* and *3* for NUB1L and FAT10, and Fig. 8*D*, *lanes 5* and *6* for GFP). We also performed this experiment with FAT10 and NUB1L expressed together by the bi-directional promoter, and found that both can be co-immunoprecipitated at the same time (Fig. 8*C*, *lane 4*). To determine the binding of the NUB1L mutants, we used NUB1L as control for NUB1LΔUBA1–3 and NUB1LΔUBL, which were all expressed from the vector pcDNA3.1. After the immunoprecipitation with MCP444, we found that NUB1LΔUBA1–3 interacted with the proteasome, but not NUB1LΔUBL (Fig. 8*C*, *lanes 5*-7). A Western blot against a subunit of the 19 S regulatory complex, Rpt6, demonstrates successful immunoprecipitation of the 26 S proteasome in all cases (Fig. 8, *E* and *F*). The ability to interact with the 26 S proteasome was shown for FAT10-N-GFP and FAT10-C-GFP in the same manner, using GFP alone as negative and FAT10-GFP as positive control (Fig. 8, *B* and *D*). The specificity of the binding was again demonstrated by the lack of co-immunoprecipitation of GFP alone, despite successful immunoprecipitation of the 26 S complex (Fig. 8*F*).

To investigate whether the interaction between FAT10 and the proteasome is direct, an *in vitro* pulldown assay was performed where recombinant GST-FAT10 was incubated together with purified 26 S proteasome. Only GST-FAT10, but not GST alone, was able to pull down the proteasome, as determined by a Western blot against the 20 S subunit iota (α1) (Fig. 8*G*) although the same amount of proteasomes was available for interaction as demonstrated by Western blotting (Fig. 8*H*).

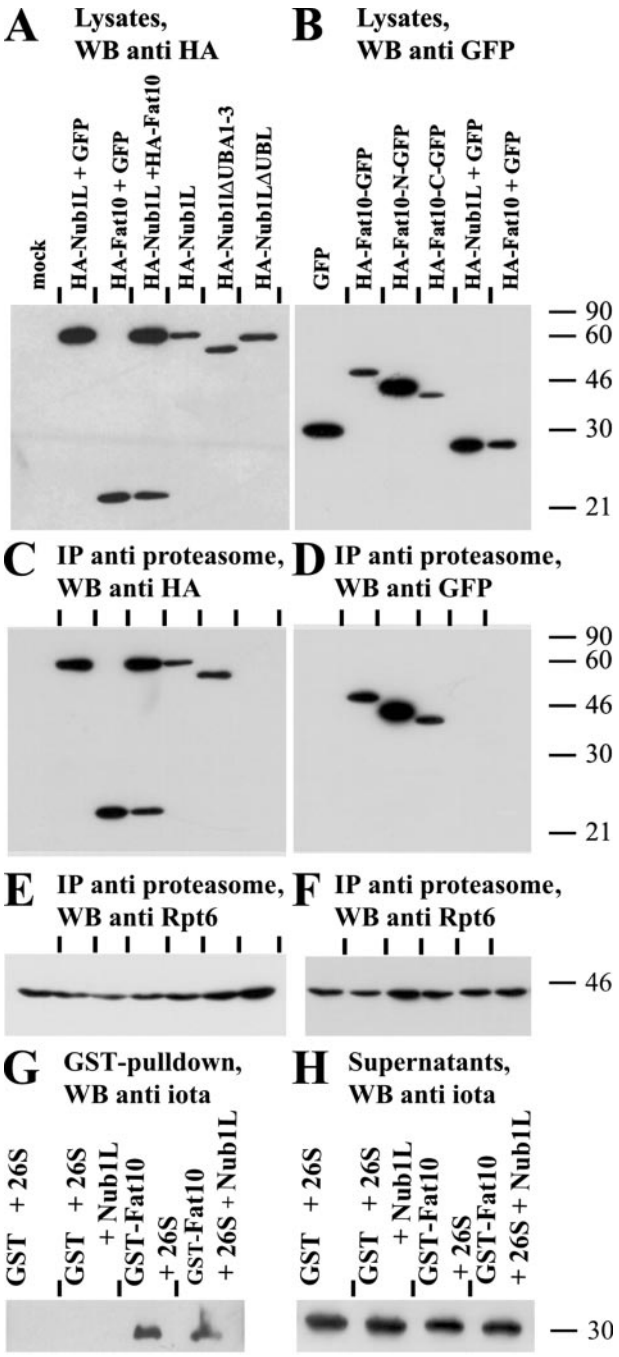

FIGURE 8. **Co-immunoprecipitation of NUB1L, NUB1LΔUBA1–3, and FAT10, but not of NUB1LΔUBL with the 26 S proteasome.** *A*, HEK293T cells were transfected with empty vector (*mock*), HA-NUB1L together with GFP (vector: pBI), HA-FAT10 together with GFP (vector: pBI), HA-NUB1L together with FAT10 (vector: pBI), HA-NUB1L (vector: pcDNA3.1), HA-NUB1LΔUBA1–3 (vector: pcDNA3.1), and HA-NUB1LΔUBL (vector: pcDNA3.1). The cells were lysed and about 2% of the lysate was analyzed by SDS-PAGE and anti-HA Western blotting (*WB*). *B*, HEK293T cells were transfected with GFP, HA-FAT10-GFP fusion protein, HA-FAT10-N-terminal UBL domain-GFP fusion protein (*HA-Fat10-N-GFP*), HA-FAT10-C-terminal UBL domain-GFP fusion protein (*HA-FAT10-C-GFP*), HA-NUB1L together with GFP (vector: pBI), and HA-FAT10 together with GFP (vector: pBI). The cells were lysed and about 2% of the lysate was analyzed by SDS-PAGE and anti-GFP Western blotting (*WB*). The positions of molecular weight markers are shown on the *right* of the gel. *C* and *D*, lysates shown in *A* and *B* were subjected to immunoprecipitation with an antibody against the 20 S proteasome subunit β7 (MCP444, anti-HN3) under conditions preserving the 26 S proteasome. The bound proteins were analyzed by Western blot with an anti-HA antibody in *C*, or with an anti-GFP antibody in *D*. The lane occupation in *C* is the same as in *A*, the lane occupation in *D* is the same as in *B*. *E* and *F*, to demonstrate the successful immunoprecipitation of the 26 S proteasome, the samples shown in *C* and *D* were also analyzed by Western blot with an antibody recognizing the 19 S regulator subunit Rpt6. The lane occupation in *E* is the same as in *A*; the lane occupation in *F* is the same as in *B*. *G*, GST pull-down experiment. GST (*lanes 1* and *2*) or GST-FAT10 (*lanes 3* and *4*) were incubated with purified 26 S proteasome in the presence or absence of recombinant His_6-NUB1L and analyzed by Western blot with an antibody recognizing the 20 S proteasome subunit iota (α1). *H*, supernatants of the GST pulldown shown in *G* were analyzed on a Western blot for iota content. The data were confirmed in three independent experiments.

TABLE 1

A summary of the results obtained

Results are classified with a plus (+) for a positive result in a binding assay or for accelerated degradation and with a minus (−) for a negative result.

	Binding to FAT10	Binding to proteasome	Accelerated degradation of FAT10
NUB1L	+	+	+
NUB1LΔUBA1–3	−	+	+
NUB1LΔUBL	+	−	−
	Binding to NUB1L	**Binding to proteasome**	**Accelerated degradation by NUB1L**
FAT10-GFP	+	+	+
FAT10-N-GFP	−	+	+
FAT10-C-GFP	+	+	+

DISCUSSION

The role of proteins that contain both a UBL domain and one or more UBA domains for the recruitment of polyubiquitylated substrates for degradation by the proteasome is currently a subject of intensive investigations (29). Whereas it was previously believed that polyubiquitylation is a sufficient label for docking to the 26 S proteasome via the subunits Rpn10 (45) or Rpt5 (46), it is now becoming clear that UBL-UBA proteins, which bind to proteasomes via their UBL domain, can be required to target a subset of ubiquitylated substrates to the proteasome thus introducing a further layer of regulation. Here we investigated the molecular interactions required for a novel proteasomal targeting system consisting of the ubiquitin-like protein FAT10 and the UBL-UBA protein NUB1L. In Table 1 we summarize the data we obtained while dissecting the different domains of NUB1L and FAT10 for interaction and accelerated degradation.

When we identified NUB1L as a non-covalent interaction partner of FAT10 that contains three *bona fide* UBA domains, it was an obvious assumption that these are required for the interaction with FAT10. Because the alternative splice variant NUB1 can be viewed as a "naturally occurring" deletion mutant of NUB1L, it appeared reasonable to delete the UBA domains singly, in pairs, and altogether. We found in GST pulldown experiments (Fig. 1*B*) and co-immunoprecipitation studies (Fig. 2) that all three UBA domains of NUB1L were required for the binding of FAT10, whereas the UBL domain was dispensable for this interaction. We were able to detect a weak interaction of FAT10 and NUB1LΔUBA3 in pulldown studies, suggesting that the combination of the first two UBA domains can mediate a weak interaction, but because this interaction was not confirmed in co-immunoprecipitation studies *in vivo*, the significance of this interaction remains uncertain. Interestingly, the

deletion of the 14 amino acids occurring in the natural splice variant NUB1 was insufficient to abolish the binding to FAT10.

While studying the interaction of isolated UBA domains with polyubiquitin chains, Raasi *et al.* (25) divided the UBA domains into four different groups, depending on their ability to discriminate between differently linked polyubiquitin chains and monoubiquitin. The members of the third group, which included all three UBA domains of NUB1L, were not able to interact with ubiquitin at all and may hence be in charge of recognizing ubiquitin-like proteins instead. Whereas most reports about UBL-UBA domain proteins focus on ubiquitin or polyubiquitylated substrates, very little is known about their interaction with ubiquitin-like modifiers. In the three first reports on this issue, NUB1 and NUB1L were found to bind to the ubiquitin-like modifier NEDD8 and to accelerate its degradation (21, 22, 43). Unexpectedly, the interaction of NUB1 and NEDD8 was not mediated by the three UBA domains but rather by a short C-terminal domain. Only the second UBA domain of NUB1L appeared to interact weakly with NEDD8 but it was not required to promote NEDD8 degradation (43). Subsequently, we reported the robust non-covalent interaction between FAT10 and NUB1L, but in the same series of experiments we failed to detect an interaction of NEDD8 and NUB1L (20). In this study we found that the concerted action of three UBA domains of NUB1L is required for the binding of FAT10, a ubiquitin-like protein containing two UBL domains.

To determine whether only one or both of the UBL domains of FAT10 are required for binding NUB1L, co-immunoprecipitation studies were performed. These experiments revealed that only the N-terminal but not the C-terminal UBL domain of FAT10 interacted with NUB1L (Fig. 6). Residues Leu^{8}, Ile^{44}, and Val^{70} of ubiquitin, known to be important for the interaction of ubiquitin with other UBA domains (27, 47–49), are only partially conserved in FAT10. The N-terminal UBL domain of FAT10 contains the Leu^{8} residue and bears a leucine in position 44, but a threonine in position 70. The C-terminal domain, in contrast, shows the corresponding residues Gly^{8}, Thr^{44}, and Ala^{70}. Whereas this seems to be in good agreement with our results, it cannot be excluded that different residues might be responsible for interaction between NUB1L and ubiquitin-like modifiers, especially because it could be shown that NUB1L does not bind a ubiquitin-GFP fusion protein (20) or polyubiquitin chains (25).

Whereas interaction of monoubiquitin with UBA domain proteins has been reported (30), usually polyubiquitylated proteins are better binders of UBL-UBA domain proteins. This can be rationalized by data on the binding affinity between ubiquitin and UBL-UBA protein Rad23, where the strength of binding increased exponentially when the chain length of ubiquitin was extended from 1 to 6 units (27). We take from our result that one of the two FAT10 UBL domains is sufficient for mediating the interaction with NUB1L (Fig. 6) as further support for the specificity of this interaction. Our data suggest that this interaction is not merely a result of an increase in avidity by connecting two ubiquitin-like domains and thus mimicking a short polyubiquitin chain. Nevertheless, because the binding assays performed in our study are of qualitative rather than quantitative nature, we cannot rule out that FAT10 or FAT10-GFP bind with a higher affinity than FAT10-N-GFP.

Several reports about the influence of UBL-UBA proteins on degradation have already appeared. The deletion of these proteins lead to an inhibition of degradation and accumulation of high molecular weight ubiquitin conjugates (30–34). Conversely, overexpression of Rad23 or Dsk2 lead to inhibition of substrate turnover by the 26 S proteasome (36, 37), and Rad23 inhibited the *in vitro* degradation of Ub_5DHFR (38). With respect to the function of UBA-UBL proteins in degradation it was proposed that they could operate as inhibitors of multiubiquitin chain assembly (37), inhibitors of deubiquitylation (38), linkers to the proteasome, and substrate carriers (30). A careful investigation based on the reconstitution of Rad23- and Rpn10-deficient proteasomes with recombinant proteins and analysis of the degradation of different substrates clearly showed a substrate specificity of the UBL-UBA proteins beyond the modification with polyubiquitin (39). This study demonstrated that deletion of a specific UBL-UBA protein lead to a slow down but not to a complete inhibition of the proteolysis of some substrates, but left others unaffected. However, in all cases the effect of the UBL-UBA protein was strictly dependent on the presence of the UBA domain.

Here we report the unexpected finding that the accelerated degradation of FAT10 by NUB1L is independent of all three of its UBA domains. Because FAT10 and NUB1LΔUBA1–3 could not be co-immunoprecipitated, this enhancement in degradation does not depend on the interaction of both proteins. Moreover, NUB1L was able to accelerate the degradation of the two isolated UBL domains of FAT10 when fused to GFP. Because only the N-terminal UBL domain of FAT10 bound to NUB1L (Fig. 6), this is the second independent experiment in which we found no correlation between the ability of NUB1L to bind a FAT10 variant and to accelerate its degradation. Therefore, a role of NUB1L as a proteasomal receptor for FAT10 cannot be the only mode of action. Because FAT10 degradation occurs also independently of ubiquitylation (19), a role for NUB1L in the protection from deubiquitylation is unlikely as well. Also a protection from putative FAT10-specific proteases is unlikely, because we failed to obtain evidence for their existence in two independent cell lines in the presence or absence of IFN-γ (19). In our experiments, the ability of NUB1L to accelerate FAT10 degradation relied solely on the UBL domain-dependent interaction with the 26 S proteasome, because both NUB1L and NUB1LΔUBA1–3 had a similar effect on the degradation rate of FAT10, whereas NUB1LΔUBL was ineffective (Fig. 3). Given that NUB1L and FAT10 can bind independently to the 26 S proteasome (Fig. 8), we favor the hypothesis that binding of NUB1L to the 26 S proteasome with its N-terminal UBL domain induces a conformational change in the 19 S regulator that favors the binding and/or degradation of FAT10 and FAT10-conjugated proteins at an independent docking site. This scenario would be analogous to the one suggested by Verma *et al.* (39) who showed that binding of the VWA domain of Rpn10 serves to facilitate the degradation of polyubiquitylated substrates delivered by Rad23. To address this hypothesis for NUB1L and FAT10, it will be important to map the binding site of FAT10 at the 26 S proteasome.

Curiously, the mutant FAT10-N-GFP is quite a stable protein (Fig. 7*A*), despite its ability to interact with the proteasome (Fig. 8*D*). Degradation of FAT10-N-GFP, however, can be readily induced by coexpression of NUB1L. These results combined argue against the recently proposed model that mere binding to the proteasome is sufficient to target for proteasomal degradation (50). Verma *et al.* (39) found that the polyubiquitylated proteasome substrate Sic1 bound to the Rpn10-deficient 26 S proteasomes in dependence of Rad23, but no degradation was observed. Thus binding seems to be a necessary but not a sufficient prerequisite for proteasomal degradation of at least some substrates. For the proteolysis of such substrates like Sic1 or FAT10, the binding of their respective facilitators Rpn10 or NUB1L to the proteasome appears to be important.

Acknowledgments—We thank Elisabeth Naidoo for excellent technical support and Selina Khan for contributing a preparation of 26 S proteasome. Klaus Hendil, Klaus Scherrer, and Michael E. Cheetham are acknowledged for the contribution of antibodies.

REFERENCES

1. Pickart, C. M. (2001) *Annu. Rev. Biochem.* **70,** 503–533
2. Hicke, L. (2001) *Cell* **106,** 527–530
3. Jesenberger, V., and Jentsch, S. (2002) *Nat. Rev. Mol. Cell Biol.* **3,** 112–121
4. Lai, E. C. (2002) *Curr. Biol.* **12,** R74–R78
5. Ma, Y., and Hendershot, L. M. (2001) *Cell* **107,** 827–830
6. Koepp, D. M., Harper, J. W., and Elledge, S. J. (1999) *Cell* **97,** 431–434
7. Jentsch, S., and Pyrowolakis, G. (2000) *Trends Cell Biol.* **10,** 335–342
8. Yeh, E. T., Gong, L. M., and Kamitani, T. (2000) *Gene* (*Amst.*) **248,** 1–14
9. Matunis, M. J., Coutavas, E., and Blobel, G. (1996) *J. Cell Biol.* **135,** 1457–1470
10. Muller, S., Hoege, C., Pyrowolakis, G., and Jentsch, S. (2001) *Nat. Rev. Mol. Cell. Biol.* **2,** 202–210
11. Osaka, F., Saeki, M., Katayama, S., Aida, N., Tohe, A., Kominami, K., Toda, T., Suzuki, T., Chiba, T., Tanaka, K., and Kato, S. (2000) *EMBO J.* **19,** 3475–3484
12. Ritchie, K. J., Hahn, C. S., Kim, K. I., Yan, M., Rosario, D., Li, L., delaTorre, J. C., and Zhang, D. E. (2004) *Nature Med.* **10,** 1374–1378
13. Kim, K. I., Malakhova, O. A., Hoebe, K., Yan, M., Beutler, B., and Zhang, D. E. (2005) *J. Immunol.* **175,** 847–854
14. Raasi, S., Schmidtke, G., Giuli, R. D., and Groettrup, M. (1999) *Eur. J. Immunol.* **29,** 4030–4036
15. Liu, Y., Pan, J., Zhang, C., Fan, W., Collinge, M., Bender, J. R., and Weissman, S. M. (1999) *Proc. Natl. Acad. Sci. U. S. A.* **96,** 4313–4318
16. Raasi, S., Schmidtke, G., and Groettrup, M. (2001) *J. Biol. Chem.* **276,** 35334–35343
17. Fan, W., Cai, W., Parimoo, S., Lennon, G. G., and Weissman, S. M. (1996) *Immunogenetics* **44,** 97–103
18. Johnson, E. S., Bartel, B., Seufert, W., and Varshavsky, A. (1992) *EMBO J.* **11,** 497–505
19. Hipp, M. S., Kalveram, B., Raasi, S., Groettrup, M., and Schmidtke, G. (2005) *Mol. Cell. Biol.* **25,** 3483–3491
20. Hipp, M. S., Raasi, S., Groettrup, M., and Schmidtke, G. (2004) *J. Biol. Chem.* **279,** 16503–16510
21. Kamitani, T., Kito, K., Fukuda-Kamitani, T., and Yeh, E. T. H. (2001) *J. Biol. Chem.* **276,** 46655–46660
22. Kito, K., Yeh, E. T. H., and Kamitani, T. (2001) *J. Biol. Chem.* **276,** 20603–20609
23. Schauber, C., Chen, L., Tongaonkar, P., Vega, I., Lambertson, D., Potts, W., and Madura, K. (1998) *Nature* **391,** 715–718
24. Hofmann, K., and Bucher, P. (1996) *Trends Biochem. Sci.* **21,** 172–173
25. Raasi, S., Varadan, R., Fushman, D., and Pickart, C. M. (2005) *Nat. Struct. Mol. Biol.* **12,** 708–714
26. Miller, R. D., Prakash, L., and Prakash, S. (1982) *Mol. Gen. Genet.* **188,** 235–239
27. Raasi, S., Orlov, I., Fleming, K. G., and Pickart, C. M. (2004) *J. Mol. Biol.* **341,** 1367–1379
28. Biggins, S., Ivanovska, I., and Rose, M. D. (1996) *J. Cell Biol.* **133,** 1331–1346
29. Miller, J., and Gordon, C. (2005) *FEBS Lett.* **579,** 3224–3230
30. Wilkinson, C. R., Seeger, M., Hartmann Petersen, R., Stone, M., Wallace, M., Semple, C., and Gordon, C. (2001) *Nat. Cell Biol.* **3,** 939–943
31. Chen, L., and Madura, K. (2002) *Mol. Cell. Biol.* **22,** 4902–4913
32. Funakoshi, M., Sasaki, T., Nishimoto, T., and Kobayashi, H. (2002) *Proc. Natl. Acad. Sci. U. S. A.* **99,** 745–750
33. Rao, H., and Sastry, A. (2002) *J. Biol. Chem.* **277,** 11691–11695
34. Saeki, Y., Saitoh, A., Tohe, A., and Yokosawa, H. (2002) *Biochem. Biophys. Res. Commun.* **293,** 986–992
35. Lambertson, D., Chen, L., and Madura, K. (1999) *Genetics* **153,** 69–79
36. Kleijnen, M. F., Shih, A. H., Zhou, P. B., Kumar, S., Soccio, R. E., Kedersha, N. L., Gill, G., and Howley, P. M. (2000) *Mol. Cell.* **6,** 409–419
37. Ortolan, T. G., Tongaonkar, P., Lambertson, D., Chen, L., Schauber, C., and Madura, K. (2000) *Nat. Cell Biol.* **2,** 601–608
38. Raasi, S., and Pickart, C. M. (2003) *J. Biol. Chem.* **278,** 8951–8959
39. Verma, R., Oania, R., Graumann, J., and Deshaies, R. J. (2004) *Cell* **118,** 99–110
40. Hendil, K. B., Kristensen, P., and Uerkvitz, W. (1995) *Biochem. J.* **305,** 245–252
41. Khan, S., Zimmermann, A., Basler, M., Groettrup, M., and Hengel, H. (2004) *J. Virol.* **78,** 1831–1842
42. Moradpour, D., Grabscheid, B., Kammer, A. R., Schmidtke, G., Groettrup, M., Blum, H. E., and Cerny, A. (2001) *Hepatology* **33,** 1282–1287
43. Tanaka, T., Kawashima, H., Yeh, E. T. H., and Kamitani, T. (2003) *J. Biol. Chem.* **278,** 32905–32913
44. Bates, E. F., Ravel, O., Dieu, M. C., Ho, S., Guret, C., Bridon, J. M., AitYahia, S., Briere, F., Caux, C., Banchereau, J., and Lebecque, S. (1997) *Eur. J. Immunol.* **27,** 2471–2477
45. van Nocker, S., Sadis, S., Rubin, D. M., Glickman, M., Fu, H., Coux, O., Wefes, I., Finley, D., and Vierstra, D. (1996) *Mol. Cell. Biol.* **16,** 6020–6028
46. Lam, Y. A., Lawson, T. G., Velayutham, M., Zweier, J. L., and Pickart, C. M. (2002) *Nature* **416,** 763–767
47. Vijay-Kumar, S., Bugg, C. E., and Cook, W. J. (1987) *J. Mol. Biol.* **194,** 531–544
48. Beal, R., Deveraux, Q., Xia, G., Rechsteiner, M., and Pickardt, C. (1996) *Proc. Natl. Acad. Sci. U. S. A.* **93,** 861–866
49. Sloper Mould, K. E., Jemc, J. C., Pickart, C. M., and Hicke, L. (2001) *J. Biol. Chem.* **276,** 30483–30489
50. Janse, D. M., Crosas, B., Finley, D., and Church, G. M. (2004) *J. Biol. Chem.* **279,** 21415–21420